J. Mol. Model. **1996**, *2*, 136 – 148

Journal of Molecular Modeling

Molecular Parameterisation and the Theoretical Calculation of Electrode Potentials

David R. Lowis[1] and W. Graham Richards*

Oxford Centre for Molecular Sciences and Physical Chemistry Laboratory, South Parks Road, Oxford OX1 3QZ, U.K. Tel: (01865) 275406. Fax: (01865) 275410. (gr@vax.ox.ac.uk)

1. Present address: Centre for Molecular Design, Washington University School of Medicine, 700 S. Euclid Ave. St Louis, MO 63110-1012, U.S.A. Tel: (314) 362-2272. Fax: (314) 362-0234. (dave@ibc.wustl.edu)

Received: 2 January 1996 / Accepted: 2 May 1996 / Published: 28 May 1996

Abstract

The difference in reduction potentials between ortho and para-benzoquinones has been calculated. The employs gas phase *ab initio* and semi-empirical computations in combination with free energy perturbation theory applied to gas and solution phase Monte Carlo simulations. The effects on calculated results of altering solute electrostatic parameterisation in solution phase simulations is examined. Atom centred charges derived from the molecular electrostatic potentials, MEPs, from optimised *ab initio* wavefunctions and charges generated by consideration of hydrogen bonded complexes are considered. Parameterisation of hydroxyl torsions in hydroquinone molecules is treated in a physically realistic manner. The coupled torsional system of the ortho-hydrobenzoquinone molecule is described by a potential energy surface calculated using gas phase AM1 semi-empirical computations rather than the simple torsional energy functions frequently employed in such calculations. Calculated differences in electrode potentials show that the electrostatic interactions of quinone and hydroquinone molecules in aqueous solution are not well described by atom centred charges derived from *ab initio* calculated MEPs. Moreover, results in good agreement with the experimental reduction potential difference can be obtained by employing high level *ab initio* calculations and solution phase electrostatic parameters developed by consideration of hydrogen bonded complexes.

Keywords: Electrode Potential, Electrostatic parameters, Quinone, Free energy perturbation, *ab initio*, Semi Empirical

Introduction

The use of Monte Carlo [1] (MC) and molecular dynamics [2] (MD) statistical mechanical simulations has become increasingly widespread and routine in the study of biomolecular and organic systems. Such methods suffer from two fundamental problems: the extent of configurational space searched and the representation of system energetics through classical potential energy functions [2] and their associated parameters. Many methods, such as umbrella sampling [3], preferential sampling [4] and double wide sampling [5] have been employed to alleviate the problem of non-ergodic phase space searching. Due to limitations in computational power, molecular mechanics force fields used to represent both inter and intramolecular interactions are still simplistic in their functional form. Much effort has been expended in the development of so called transferable parameters [6 - 10] used to characterise non-bonded van der Waals and electrostatic interactions. Such parameterisations have met with some

* *To whom correspondence should be addressed*

success in the calculation of solution phase physical properties. Nevertheless, the reliability and transferability of parameter sets between different systems must still be considered questionable, especially with respect to the atom centred charges used to represent electrostatic interactions.

Intermolecular interactions in most commonly used force fields comprise electrostatic and Lennard-Jones van der Waals terms [8 - 10] Non-bonded electrostatics are, in general, represented as simple coulombic interactions between point charges placed on atomic centres. Such atom centred charges may be derived in a number of different ways. This paper investigates the effects on calculated quinone redox potentials of changing molecular electrostatic parameterisation used in MC simulations in order to assess the quality of the parameters used. Redox potential results calculated using atom centred charges obtained from 1) fitting to *ab initio* computed molecular electrostatic potentials (MEPs) [11] and 2) those obtained by considering hydrogen bonded complexes of the quinones are their respective hydroquinones, an OPLS methodolgy [7], are compared.

The difference in reduction potentials between ortho and para-benzoquinones is calculated using a combination of gas phase *ab initio*, semi-empirical and solution and gas phase MC simulations. Free energy perturbation [12] (FEP) theory is used in the calculation of solution phase free energy differences. The quinone system was selected because of the availability of experimental data [13], the relative simplicity of the systems involved and the fact that anthraquinone compounds are likely candidates for bioreductive anti-cancer agents [14]. Additionally, an earlier study[15], which employed a similar methodology but utilised MD simulations, calculated the difference in redox potentials between these compounds to an apparent accuracy of 20mV. The problem of torsional parameterisation in flexible molecules is also addressed. The coupled torsional system of ortho-hydrobenzoquinone is parameterised to a semi-empirically calculated potential energy surface rather than the more usual simple torsional energy functions.

Methods

A simple thermodynamic cycle (figure 1) approach was used to calculate the difference in electrode potentials between ortho and para-benzoquinones. The difference in standard reduction potentials between ortho and para-benzoquinones, ΔE, is related to this solution phase free energy difference $\Delta\Delta G_{aq}$ by equation 1.

$$\Delta\Delta G_{aq} = -nF(\Delta E^{o}) \qquad (1)$$

where n is the number of electrons involved in the redox process, F is Faraday's constant and ΔE^{o} the difference in reduction potentials between ortho and para-benzoquinones.

The aqueous phase free energy term $\Delta\Delta G_{aq}$ may be calculated from the thermodynamic cycle employing Hess' law (equation 2).

$$\Delta\Delta G_{aq} = \Delta\Delta G_{gas} + (\Delta G_{3} - \Delta G_{1}) - (\Delta G_{2} - \Delta G_{4}) \qquad (2)$$

see figure 1 for explanation of terms.

$\Delta\Delta G_{gas}$ represents the gas phase free energy difference between the ortho-hydrobenzoquinone / para-benzoquinone system (top left of cycle) and the ortho-benzoquinone / para-hydrobenzoquinone system (top right of cycle). Terms ΔG_{3} - ΔG_{1} and ΔG_{2} - ΔG_{4} represent the differences in the solvation free energies between the reduced and oxidised forms of ortho and para-benzoquinones respectively

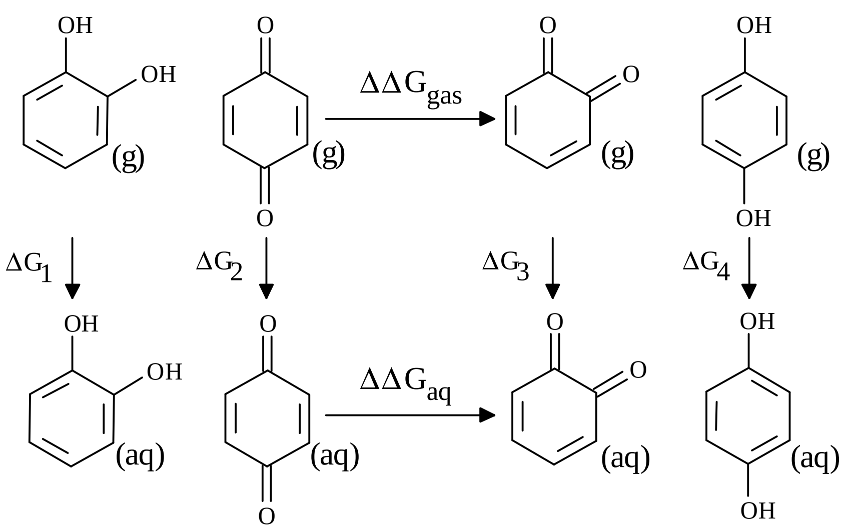

Figure 1. *Thermodynamic cycle used to calculate the difference in reduction potentials between ortho and para-benzoquinones.*

Calculation of the gas phase free energy difference, $\Delta\Delta G_{gas}$. The quantity $\Delta\Delta G_{gas}$, can be constructed from a number of terms as depicted in equation 3.

$$\Delta\Delta G_{gas} = \Delta\Delta H_{0K} + \Delta\Delta H_{ZPE} + \Delta\Delta H_{thermal} + T\Delta\Delta S \quad (3)$$

explanation of terms in text.

$\Delta\Delta H_{0K}$ is the difference in gas phase internal energies at 0K. This quantity was computed using *ab initio* calculations employing the Gaussian 92 program [16]. Full restricted Hartree-Fock (RHF) geometry optimisations were carried out on ortho- and para-benzoquinones and their respective hydroquinones at the STO-3G [17], 3-21G [18] and 6-31G* [19] basis set levels. All computations involved the calculation of atom centred charges through the CHELPG [11] algorithm in order to provide molecular electrostatic parameters for the solution phase simulations. Finally MP2/6-31G*]20] single point calculations were performed on the RHF/ 6-31G* optimised geometries to obtain accurate gas phase energies and therefore $\Delta\Delta H_{0K}$. The quantities $\Delta\Delta H_{ZPE}$, the difference in molecular zero point energies, $\Delta\Delta H_{thermal}$, the difference in molecular thermal enthalpies, and $T\Delta\Delta S$, the difference in molecular entropies at 298K, were obtained from gas phase semi-empirical calculations. Single pointAM1 [21] calculations were run on the RHF/6-31G* optimised molecular geometries of all quinone and hydroquinone species in order to obtain normal vibrational frequency modes and thermodynamic quantities ($\Delta\Delta H_{thermal}$, and $T\Delta\Delta S$). Analysis of the computed vibrational frequency modes through equation 4 produced molecular zero point energies which, along with the calculated thermodynamic quantities were used to correct the *ab initio* calculated 0K internal energies to free energies at 298K (equation 3). All semi-empirical calculations were run using the MOPAC [22] program, version 6.

$$Z.P.E. = 0.5\ h\ \Sigma_i\ \omega_i / 2\pi \quad (4)$$

where Z.P.E. is the molecular zero point energy, h is Planck's constant and ω_i the normal vibrational modes of the molecule.

The calculation of $\Delta\Delta G_{gas}$ through equation 3 is valid only if the molecules are assumed to maintain a rigid geometry. The energy barriers to internal rotation for the hydroxyl groups of the hydroquinones are, however, low in comparison with available thermal energy at 298K [13]. Thus, representation of the hydroquinones as rigid molecules in both the gas and solution phase is physically unrealistic.The contribution made to $\Delta\Delta G_{gas}$ by variation in hydroquinone hydroxyl torsions was found from MC simulations and FEP theory.

Gas phase mutations of ortho-hydrobenzoquinone to ortho-benzoquinone and para-hydrobenzoquinone to para-benzoquinone were performed (see figure 2) and the free energy changes calculated using FEP theory. Each perturbation was divided into 21 windows [23] to allow the precise evaluation and rapid convergence of calculated free energy changes. The progress of the perturbations was described by a coupling parameter, λ, the hydroquinone being described by $\lambda = 0$ and the quinone by $\lambda = 1$ and the perturbation between the two by l being increased from 0 to 1 in increments of 0.05. Each of the mutations was performed in a series of 22 MC simulations designed to give two estimates (forward, hydroquinone -> quinone, and backward, quinone -> hydroquinone) of the gas phase free energy change. Both quinones and hydroquinones were represented by all atom models in their RHF/3-21G optimised. Quinone molecules were treated as rigid moieties. Only hydroquinone torsional degrees of freedom were sampled and only torsional contributions to the free energy changes were evaluated. Details of the hydroquinone torsional parameterisation can be found in the later section dealing with the subject. Metropolis sampling [1] was employed throughout all simulations. Dihedral angles were allowed to vary by up to 10^o per MC step in order to allow an acceptance ratio for torsional moves of around 40%. All simulations were run using the BOSS program, version 3.1 [24], on a Hewlett Packard workstation. Each simulation consisted of 10×10^3 configurations of equilibration the first 3×10^3 of which were at constant volume, followed by 16×10^3 configurations of data collection. All simulations were run in the isothermal-isobaric ensemble at 298 K and 1 atmosphere pressure.

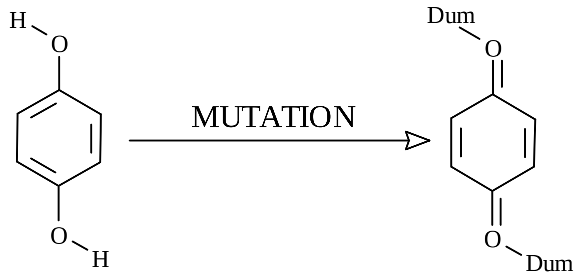

Figure 2. *Mutation of para-hydrobenzoquinone to the quinone. During the mutation parameters which describe the hydroquinone, bond lengths, angles, dihedrals and van der Waals and electrostatic parameters are slowly changed to those which describe the quinone. Hydroquinone hydroxyl hydrogen atoms are shrunk into massless, chargeless dummy atoms, denoted Dum in the figure.*

Calculation of solution phase free energy differences

The differences in the free energies of solvation between the hydroquinones and the quinones, $\Delta G_3 - \Delta G_1$ and $\Delta G_2 - \Delta G_4$ for ortho and para systems respectively, were calculated employing MC statistical mechanics simulations and free energy perturbation theory. The difference in solvation free energies between ortho-and ortho-benzoquinone was computed by mutating the hydroquinone to the quinone (figure

2) in dilute aqueous solution. Application of the FEP equation [25] (equation 5) to collated simulation data was used to calculate the free energy change. A similar computation was performed for the para-quinone system

$$\Delta G = -kT \ln \langle \exp(-\Delta H_{AB}/ kT) \rangle_A \qquad (5)$$

the FEP equation. k is Boltzmanns constant, T the temperature, ΔH_{AB} the difference in internal energies between systems A and B both being in the same configurational state. The brackets $\langle\rangle_A$ represent an average taken over configurations of state A.

Differences in solvation free energies comprise contributions from two sources: changes in intermolecular interactions upon solvation and changes in intramolecular interactions upon solvation of the species involved. This second quantity, which involves the polarisation of solute molecules by solvent, is notoriously difficult to calculate and has been ignored in this study. Hence, all solution phase simulations involved the evaluation of intermolecular energies only. Intramolecular interactions are described in the BOSS program in the usual Lennard-Jones plus Coulombic format (equation 6).

$$\Delta E = \Sigma_i^a \Sigma_j^b \left(A_{ij}/r^{12}_{ij} - C_{ij}/r^6_{ij} + q_i q_j \varepsilon^2/r_{ij}\right) \qquad (6)$$

explanation of terms in text.

The interaction energy between two molecules is thus characterised by the sum over all pairwise interactions between atoms i and j on the two molecules a and b. The terms A and C in equation 6 are related to the Lennard-Jones e and s parameters such that $A_{ii} = 4\varepsilon_i\sigma^{12}_i$ and $C_{ii} = 4\varepsilon_i\sigma^6_i$. s and e Lennard Jones parameters for all atoms were taken from the OPLS force field [6].

Intermolecular electrostatic interactions are represented in the BOSS program as coulombic interactions between point charges placed on atom centres. Atom centred charges computed in the RHF *ab initio* calculations described in the previous section were used to provide three sets (STO-3G, 3-21G and 6-31G*) of electrostatic parameters for each molecule. In addition to these a further set of electrostatic parameters was specially developed for the quinone system through the consideration of hydrogen bonded complexes of the quinone and hydroquinone molecules. This method is comparable to that used to develop OPLS parameters for the nucleotide bases [7].

Electrostatic parameter development

OPLS parameters for both united and all atom representations have been derived through pure liquid simulations [6] and reproduction of *ab initio* calculated geometries and binding energies of hydrogen bonded complexes of the solutes in question [7]. It was decided to use this second, simpler approach to derive electrostatic parameters for the quinone / hydroquinone molecules under study. 11 hydrogen bonded complexes (figure 3) of the four molecules involved were considered. Binding energies for these complexes were obtained from RHF/6-31G* *ab initio* calculations. A full restricted Hartree-Fock geometry optimisation of a single water molecule was performed at the 6-31G* basis set level. Hartree-Fock geometry optimisations of the hydrogen bond lengths and angles of complexes A through K were performed at the 6-31G* basis set level. All other internal coordinates were held fixed at the values obtained from RHF/6-31G* optimisations of the isolated molecules. It should be noted that RHF/6-31G* and RHF/3-21G optimised molecular geometries are practically identical.

In the case of the quinone molecules themselves only one hydrogen bonded complex exists for each (A and B, figure 3). It is therefore possible to reproduce hydrogen bond geometries and energies of these complexes with many different sets of atom centred charges. In order to combat this effect quinone-water complexes were set up with an OH water bond in direct line with the O=C carbonyl bond of the quinone. RHF/6-31G* optimisations of the bond length only were performed on these complexes, denoted A2 and B2, to provide second quinone complexes which could be used in the parameterisation process. Binding energies for the hydrogen bonded complexes were obtained by subtracting the RHF/6-31G* energies of the isolated constituent molecules from the RHF/6-31G* energy of the optimised complex.

In order to reproduce *ab initio* calculated geometry and binding energy data using atom centred charges, the hydrogen bond lengths and angles of complexes A through K were optimised employing the BOSS intermolecular potential function (equation 6). This process was performed using the SOPLS program [26] which employs a simplex minimisation method. Output from the SOPLS code includes the complex energy, optimised geometry as well as coulombic and van der Waals interaction energies between individual atom pairs. A directed trial and error procedure was utilised to obtain electrostatic parameters which yielded hydrogen bond geometries and binding energies for complexes A through K in good agreement with the *ab initio* calculated values.

The hydrogen bond lengths and angles of complexes A through K and the hydrogen bond lengths of complexes A2 and B2 were minimised using the SOPLS program. Quinone and hydroquinone molecules were represented in their RHF/6-31G* optimised geometry with initial electrostatic parameters being taken as Mulliken charges obtained from the RHF/6-31G* *ab initio* calculations on the isolated molecules. OPLS parameters were employed to represent van der Waals interactions throughout. Water was represented as the TIP4P model [27] which was to be used in the solution phase simulations. Only intermolecular interactions were evaluated. Quinone and hydroquinone electrostatic parameters were altered based on the results of these minimisations using individual atom pair interaction energies as a guide. This process was repeated until agreement in hydrogen bond geometries and interaction energies between the *ab initio* and SOPLS calculations

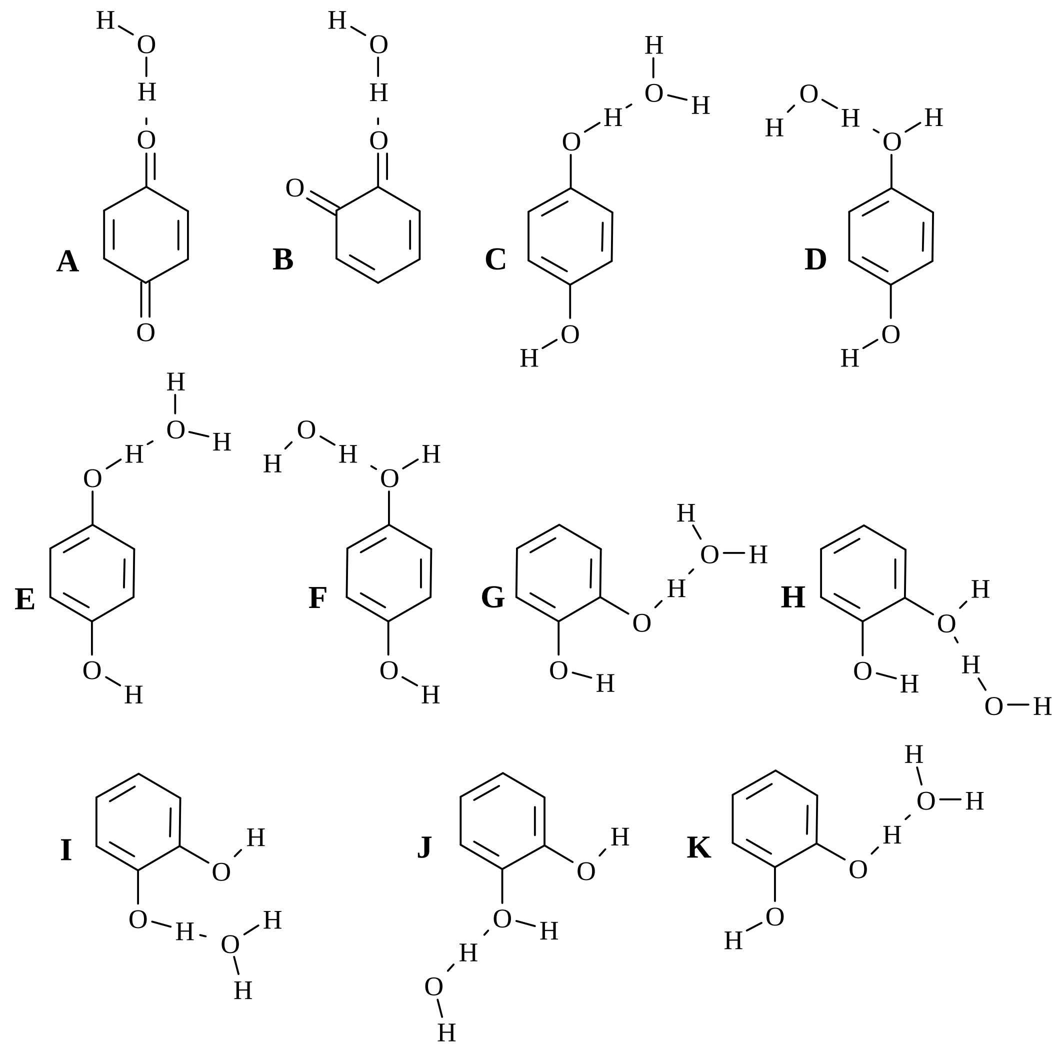

Figure 3. *Complexes used in the derivation of optimised electrostatic parameters for ortho and para benzoquinones and hydrobenzoquinones. Hydrogen bond angles were defined as the angle between the atoms water oxygen, water hydrogen and quinone/hydroquinone oxygen where water acts as a hydrogen bond donor and between atoms water hydrogen, water oxygen and hydroquinone hydrogen where water acts as a hydrogen bond acceptor.*

over all complexes could no longer be improved. Values of OPLS electrostatic parameters for atoms in chemically similar environments to those in the quinone and hydroquinone molecules were used as a check on the parameters obtained to ensure there were no drastic discrepancies.

Torsional parameterisation

As has been mentioned, the hydroxyl torsions of ortho and para-hydrobenzoquinones have low energy barriers to rotation. It would therefore be inappropriate to employ rigid molecular geometries for their representation. The BOSS program allows for sampling over torsional degrees of freedom employing a Fourier series [28] (equation 7) to describe the energetics of the torsional system.

$$V(\phi) = V(0) + V(1)\,[1 - \cos\phi] / 2 + V(2)\,[1 - \cos 2\phi] / 2 + V(3)\,[1 + \cos 3\phi] / 3 \qquad (7)$$

where $V(\phi)$ is the torsional energy when the dihedral angle has value ϕ, V(0), V(1), V(2) and V(3) are the fourier coefficients.

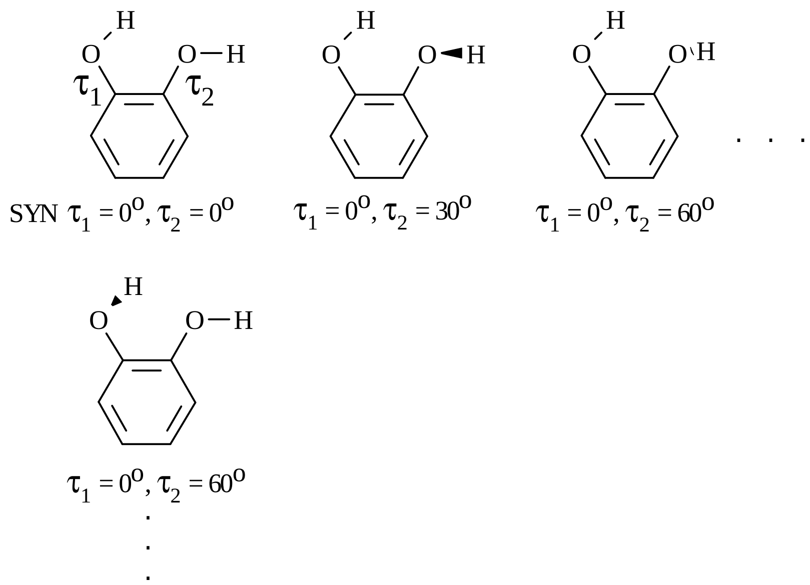

Figure 4. *Conformational forms of ortho-hydrobenzoquinone upon which AM1 semi-empirical calculations were performed in order to parameterise the coupled hydroxyl torsional system of the molecule.*

In the case of para-hydrobenzoquinone the hydroxyl groups are remote from each other and can be approximated to two isolated torsional systems. In this case the hydroxyl torsions can be described adequately by the Fourier series. In the case of ortho-hydrobenzoquinone, however, the hydroxyl torsions are situated on adjacent carbon atoms of the aromatic ring and can therefore interact producing a coupled torsion system with complex energetic behaviour. Such behaviour cannot be described adequately by the use of Fourier series which, through symmetry arguments, should be identical for each hydroxyl torsion. Furthermore, attempts to reproduce the AM1 coupled dihedral energy surface by allowing 1-4 and 1-5 intramolecular interactions between the hydroxyl groups and the hydroquinone ring atoms met with no success.

The energetic properties of the coupled hydroxyl torsion system of ortho-hydrobenzoquinone were investigated using AM1 semi-empirical calculations. Using the RHF/6-31G* geometry as a starting point, single point AM1 calculations were performed at 30° intervals of both hydroxyl torsions (τ_1 and τ_2) such that calculations were performed at $\tau_1 = 0°$ $\tau_2 = 0°$, $\tau_1 = 30°$ $\tau_2 = 0°$, $\tau_1 = 60°$ $\tau_2 = 0°$,..... $\tau_1 = 0°$ $\tau_2 = 30°$, $\tau_1 = 30°$ $\tau_2 = 30°$ ... $\tau_1 = 180°$ $\tau_2 = 180°$ (see figure 4). The resultant energy surface was used explicitly to parameterise the coupled torsion system. The BOSS source code was modified to allow it to read the torsional energy surface and interpolate between calculated points thus allowing torsional sampling directly according to the calculated energy surface.

Simulations

Ortho and para-hydrobenzoquinones were mutated to their respective quinone forms in aqueous solution. Each perturbation was split into 21 windows to allow the precise evaluation and rapid convergence of calculated free energy changes. The progress of the perturbations was described by a coupling parameter, λ, such that, the reduced quinone form being described by $\lambda = 0$, the oxidised form by $\lambda = 1$ and the perturbation from hydrobenzoquinone to benzoquinone by λ being increased from 0 to 1 in increments of 0.05.

Each mutation was performed in a series of 22 MC statistical mechanical simulations designed to give two estimates of the (forward, hydroquinone -> quinone, and backward, quinone -> hydroquinone) of the difference in solvation free energies between hydroquinone and quinone. All mutations were performed in a periodic box containing 504 water molecules. The TIP4P model was employed for interactions involving solvent whilst all quinone and hydroquinone molecules were represented by all atom models in their RHF/3-21G optimised geometries. Parameters describing van der Waals interactions were taken from the OPLS force field whilst CHELPG calculated atom centred charges calculated from the MEPs of the RHF/3-21G optimised wavefunctions were employed for electrostatic interactions. Electrostatic parameters on symmetry related atoms were taken as averaged values over those atoms. Ortho-hydrobenzoquinone torsional parameterisation was employed as described in the above section. Para-hydrobenzoquinone torsions were parameterised by setting V(2) in the BOSS Fourier series to 13.99 $kJmol^{-1}$, the experimental torsional energy barrier height for phenol [13]. Quinone molecules were treated as rigid. Each simulation consisted of 3.3×10^6 configurations of equilibration, the first 3×10^5 of which were at constant volume, followed by 6.5×10^6 configurations of data collection. These two mutations were repeated employing the optimised electrostatic parameters discussed above.

The effects of altering the electrostatic parameterisation were examined by mutating the electrostatic parameters of the reduced and oxidised forms of both ortho and para-benzoquinones from the RHF/3-21G MEP fitted charges, used

Table 1 *Results from ab initio and semi empirical gas phase calculations.*

Calculation method	Quantity	Value [$kJmol^{-1}$]
AM1 Semi-empirical	$\Delta\Delta H_{ZPE}$	0.028
	$\Delta\Delta H_{thermat}$	-0.144
	$T\ \Delta\Delta S$	-0.293
ab initio, RHF/STO-3G	$\Delta\Delta H_{0K}$	13.271
ab initio, RHF/3-21G	$\Delta\Delta H_{0K}$	45.414
ab initio, RHF/6-31G*	$\Delta\Delta H_{0K}$	46.407
ab initio, MP2/6-31G*	$\Delta\Delta H_{0K}$	40.168

in the previous structural mutations, to each of the other two *ab initio* derived electrostatic parameter sets. Each of the 8 necessary perturbations was performed in a series of 11 simulation windows designed to give two estimates (forward and backward) of the free energy change. All simulations were performed in a periodic box of 504 water molecules. The TIP4P model was employed for all solvent interactions whilst hydroquinone and quinone molecules were represented in their RHF/3-21G geometries. Van der Waals parameters for the quinone and hydroquinone molecules were taken from the OPLS force field. Free energy changes from these simulations can be combined with the free energy changes calculated from the hydroquinone to quinone mutations to evaluate the values of ΔG_3 - ΔG_1 and ΔG_2 - ΔG_4 for different electrostatic parameter sets. Each charge mutation simulation consisted of 2.3×10^6 configurations of equilibration, the first 3×10^5 of which were at constant volume, followed by 5×10^6 configurations of data collection.

Metropolis and preferential sampling were employed throughout all simulations. Spherical cutoffs for intermolecular interactions were applied at 8.5 Å for both solvent-solvent and solute-solvent interactions with the cutoff criterion such that if any atom of the solute lay within the cutoff then interactions with all solute atoms were included in the calculation. Hydroxyl torsions were allowed to vary up to 10^o per MC step. Parameters which determine the range of solute molecule movement were set in order to achieve an overall configuration acceptance rate of approximately 40%. Simulations involving the para system were run using BOSS, version 3.1 whilst those involving the ortho system were run using a version of BOSS modified to allow dihedral sampling according to the calculated AM1 energy surface.

Intramolecular contributions to all solution phase free energy changes caused by the inclusion of energy terms to represent torsional energy barriers were estimated by application of the FEP equation to dihedral angle distributions from each simulation window. These intramolecular contributions were subsequently removed from calculated solution phase free energy changes.

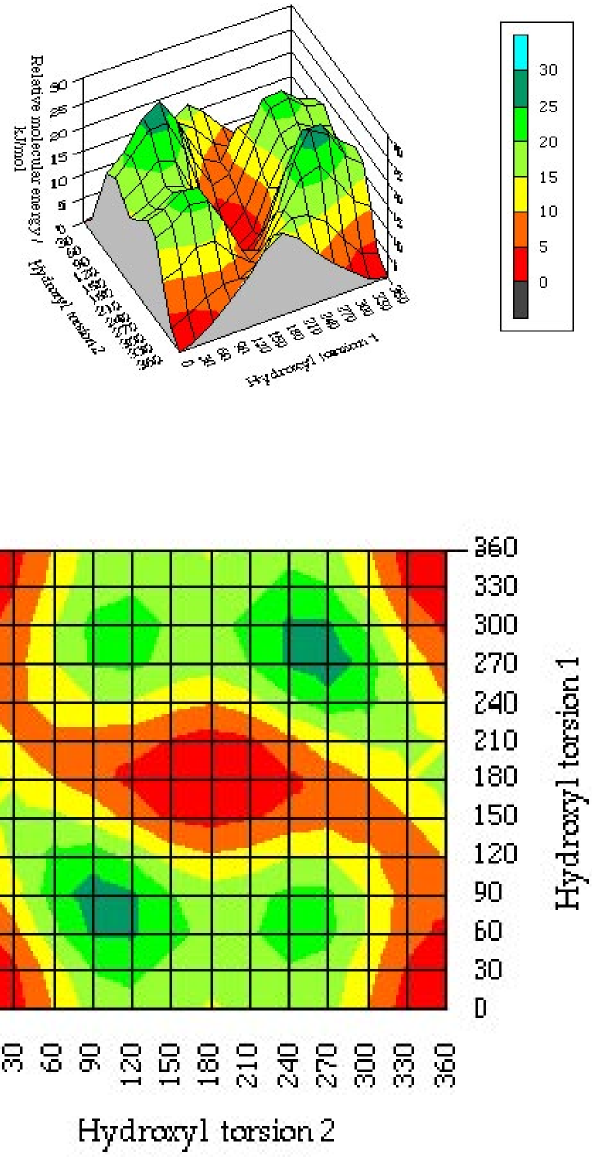

Figure 5. *3D and contour plots of the AM1 potential energy surface used to parameterise the coupled torsional system of ortho-hydrobenzoquinone.*

Results and Discussion.

Semi-empirical and ab initio gas phase

Results from the *ab initio* and semi-empirical gas phase calculations are displayed in table 1.

It can be seen from table 1 that thermodynamic quantities calculated semi-empirically, employing the AM1 hamiltonian make only a minor correction to *ab initio* gas phase energy differences. The maximum correction to $\Delta\Delta G_{gas}$ being only 0.293 $kJmol^{-1}$ for the entropic contribution. Results from the RHF/STO-3G *ab initio* calculations give markedly lower values for the difference in 0K gas phase energies than do the other basis sets. 3-21G and 6-31G* RHF computations show close agreement differing by less than 1 $kJmol^{-1}$. The effects of electron correlation, as found from the MP2/6-31G* calculations reduce the difference in gas phase energies between the species by 6.239 $kJmol^{-1}$ from the RHF/6-31G* value.

Torsional parameterisation and gas phase simulations

The results from the AM1 calculations on the conformational forms of ortho-hydrobenzoquinone are shown in figure 5 in both 3D and contour form.

The coupled dihedral energy surface and contour plots displayed show global minima at $\tau_1 = 0^o$, $\tau_2 = 0^o$ and $\tau_1 = 180^o$, $\tau_2 = 180^o$ (minima at $\tau_1 = 0^o$, $\tau_2 = 360^o$, $\tau_1 = 360^o$, $\tau_2 = 0^o$ and $\tau_1 = 360^o$, $\tau_2 = 360^o$ are identical to the $\tau_1 = 0^o$, $\tau_2 = 0^o$ global minimum). These two global minima represent the two degenerate syn forms of ortho-hydrobenzoquinone in which both hydroxyl groups point in the same direction (either to the left or the right - see figure 4). A steep sided valley running approximately (τ_1 , τ_2) $0^o, 0^o$ -> $120^o, 30^o$ -> $180^o, 120^o$ -> $180^o, 180^o$ -> $180^o, 240^o$ ->$240^o, 330^o$ -> $360^o, 360^o$ is also evident on the energy surface. This valley represents the minimum energy route for interconversion between the two degenerate syn forms of ortho-hydrobenzoquinone. The highest energy point in this valley (at approximately $\tau_1 = 150^o$, $\tau_2 = 330^o$ or $\tau_1 = 210^o$, $\tau_2 = 30^o$) corresponds to the transition state for the interconversion between the two syn forms and is some 17.2 $kJmol^{-1}$ above the syn energy minima. The valley in the energy surface demonstrates that the lowest energy path for syn-syn interconversion is available through concerted motion of the two adjacent hydroxyl groups. The conformation of the ortho-hydrobenzoquinone molecule at this saddle point correlates well with the rotational saddle point structure for the interconversion of syn forms calculated from an RHF/3-21G *ab initio* transition state search [15]. A subsidiary minimum is also observable on the energy surface at $\tau_1 = 0^o$, $\tau_2 = 180^o$ corresponding to the anti conformation (in which the hydroxyl groups ‘point’ away from each other).

Table 2 *Free energy results from the gas phase mutations hydroquinone -> quinone for both ortho and para systems.*

Mutation	$\Delta\Delta G_{torsion}$ [$kJmol^{-1}$]		
	forward	backward	average
2hpbq -> pbq	-6.86	-6.88	-6.87 ± 0.02
2hobq -> obq	-7.47	-7.49	-7.48 ± 0.02

It was this energy surface which was used to parameterise the hydroxyl torsions of ortho-hydrobenzoquinones in MC simulations. Free energy results from both gas phase mutations are given in table 2.

It can be seen from this table that free energy changes calculated from forward and backward perturbations are in excellent agreement with hystereses of less than 0.1 $kJmol^{-1}$ for both systems. Standard deviations on incremental free energy changes from each individual simulation window were small indicating good convergence the calculated quantity. The free energy change for the mutation of para-hydrobenzoquinone to para-benzoquinone in the gas phase, evaluating only torsional energy terms, is -6.87 $kJmol^{-1}$. The free energy change for the ortho mutation is -7.48 $kJmol^{-1}$. Thus the torsional contribution to $\Delta\Delta G_{gas}$ is -7.48 - (-6.87) = -0.61 $kJmol^{-1}$. Calculated values for $\Delta\Delta G_{gas}$ including the torsional contribution are displayed in table 3.

Dihedral angle distributions from para-hydrobenzoquinone perturbation showed that both hydroxyl rotational minima (where the hydroxyl group is coplanar with the aromatic ring) were sampled for both hydroxyl groups. Examination of the coupled dihedral angle distribution for ortho-hydrobenzoquinone perturbation showed that although the most sampled conformations were in and around the syn

Table 3 *Calculated values of $\Delta\Delta G_{gas}$ from gas phase ab initio, semi-empirical and gas phase perturbation calculations.*

Quantity	***ab initio* calculation**	**Value [$kJmol^{-1}$]**
$\Delta\Delta G_{gas}$ (from equation 3)	RHF/STO-3G	13.448
	RHF/3-21G	45.591
	RHF/6-31G*	46.584
	MP2/6-31G*	40.345
$\Delta\Delta G_{torsion}$		-0.61
$\Delta\Delta G_{gas}$ (including torsional contribution)	RHF/STO-3G	12.838
	RHF/3-21G	44.981
	RHF/6-31G*	45.956
	MP2/6-31G*	39.735

Table 4 *Optimised hydrogen bond binding energies and geometries calculated by both ab initio and SOPLS methods.*

Complex	*ab initio*			BOSS / SOPLS		
	Binding energy [$kJmol^{-1}$]	Hydrogen bond length [Å]	Hydrogen bong angle [°]	Binding energy [$kJmol^{-1}$]	Hydrogen bond length [Å]	Hydrogen bong angle [°]
A	-25.16	2.09	151.4	-25.20	1.76	167.3
A2	-14.87	2.13	(180.0)*	-20.72	1.75	(180.0)*
B	-25.83	2.09	152.5	-25.83	2.01	152.5
B2	-13.60	2.17	(180.0)*	-19.62	1.99	(180.0)*
C	-27.60	1.96	137.2	-27.38	2.06	144.8
D	-18.78	2.09	160.6	-19.26	1.74	175.0
E	-27.07	1.97	138.3	-27.13	2.06	147..9
F	-18.09	2.09	160.0	-18.13	1.74	174.5
G	-30.65	1.93	134.2	-30.81	2.04	130.6
H/I	-15.94	2.01	123.0	-18.50	2.12	93.6
J	-19.54	2.08	160.0	-20.22	1.78	172.4
K	-27.13	1.96	139.7	-27.00	2.04	137.0

minimum, the anti conformation and the degenerate syn conformation were also sampled.

Electrostatic parameterisation

Optimised hydrogen bond lengths, angles and binding energies found from *ab initio* and molecular mechanics (the BOSS force field, SOPLS program) are displayed in table 4.

Examination of table 4 indicates that binding energies of the complexes calculated using SOPLS are in good agreement with those calculated by *ab initio* methodology. The SOPLS calculated binding energy of the para-benzoquinone-water complex, A, differs from the *ab initio* value by only 0.04 $kJmol^{-1}$. SOPLS and *ab initio* calculated hydrogen bond lengths show a disparity of 0.33 Å and hydrogen bond angles by 15.9°. Inspection of the SOPLS calculated data for the A2 complex shows poorer agreement with *ab initio* calculated values than does the complex A. The binding energy of the A2 complex is, however, smaller than that for the A complex and so the qualitative trend in binding energies between the two has been reproduced.

SOPLS calculated binding energy and hydrogen bond geometry data for the ortho-benzoquinone-water complex, B, show excellent agreement with the *ab initio* calculated values. Calculated binding energies and hydrogen bond angles are identical to two and one decimal places respectively whilst the SOPLS calculated hydrogen bond length is only 0.08 Å shorter than the *ab initio* calculated value. As in the case of the para-benzoquinone-water complexes, A and A2, agreement between SOPLS and *ab initio* calculated binding energies and hydrogen bond geometry for the B2 complex is poorer than for the B complex. Again, however, the trend in binding energies between B and B2 complexes is qualitatively reproduced.

Binding energies of complexes D, F and J (where water acts as a hydrogen bond donor) calculated through SOPLS all lie in the range -21.0 $kJmol^{-1}$ to -18.0 $kJmol^{-1}$ compared with the range -20.0 $kJmol^{-1}$ to -18.0 $kJmol^{-1}$ for *ab initio* optimised complexes. The average discrepancy between SOPLS and *ab initio* calculated binding energies for complexes D, J and F is only 0.37 $kJmol^{-1}$. Although SOPLS calculated binding energies show excellent agreement with *ab initio* calculated values, SOPLS hydrogen bond lengths are all shorter than their *ab initio* counterparts by 0.33 Å on average. SOPLS calculated hydrogen bond lengths for complexes D, F and J show excellent agreement with each other matching the observed *ab initio* trend. Hydrogen bond angles calculated using SOPLS for complexes D, F and J are all within 3° of each other, a trend seen in the *ab initio* results. SOPLS hydrogen bond angles for these complexes, however, tend to be larger than the *ab initio* calculated values by approximately 14°.

It should be noted that in both the *ab initio* optimisations and the SOPLS minmisations complexes H and I converge on the same hydrogen bonded structure with water acing as a hydrogen bond acceptor. The H / I complex shows the poorest agreement between SOPLS and *ab initio* calculated binding energies and hydrogen bond geometries within the hydroquinone complexes. The ortho-hydrobenzoquinone-water binding energy in this complex differs between the two

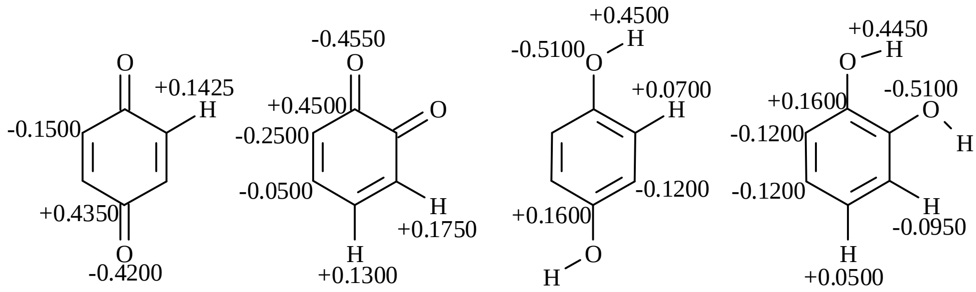

Figure 6. *Optimised electrostatic parameters for ortho and para benzoquinones and hydrobenzoquinones.*

calculation methods by 2.56 kJmol^{-1} whilst hydrogen bond length and angle differ by 0.11 Å and 29.4°. Although this agreement is relatively poor the SOPLS calculated binding energy is lower than all but the F complex and the hydrogen bond angle is the smallest out of all complexes. This is in reasonable agreement with the trends seen in the *ab initio* calculated values.

The SOPLS and *ab initio* calculated binding energies for complexes C, E, G, and K (where water acts as a hydrogen bond acceptor) all show close agreement with the average difference being 0.143 kJmol^{-1} . The largest discrepancy in these figures is 0.22 kJmol^{-1} for the C complex. The trend in *ab initio* calculated binding energies for these complexes is also reproduced in the SOPLS calculations; the binding energies of complexes C, E and K all lie in the range -28.0 kJmol^{-1} to -27.0 kJmol^{-1} with the G complex having the largest binding energy of -30.65 kJmol^{-1}. Hydrogen bond lengths for complexes C, E, G and K calculated through SOPLS are larger in magnitude than the *ab initio* calculated values by approximately 0.1 Å. SOPLS calculated hydrogen bond angles for complexes C, E, G and F all show reasonable agreement with *ab initio* calculated values.

With the exception of A2, B2 and H/I complexes, SOPLS binding energies show remarkably good agreement with those calculated using *ab initio* methodology. Hydrogen bonded geometries calculated using SOPLS show deviation from *ab initio* calculated values, however, discrepancy is not large and many of the trends seen in the *ab initio* results are reproduced. The average differences between *ab initio* and SOPLS calculated binding energies are 2.95 kJmol^{-1} for para-benzoquinone complexes, 3.01 kJmol^{-1} for ortho-benzoquinone complexes, 0.20 kJmol^{-1} for para-hydrobenzoquinone complexes and 0.88 kJmol^{-1} for ortho-hydrobenzoquinone complexes. Thus, although the results of the SOPLS calculations on complexes A through K do not agree perfectly with the *ab initio* results it can be asserted that the use of the optimised electrostatic parameters in conjunction with OPLS van der Waals parameters do adequately represent intermolecular quinone and hydroquinone interactions with the respect to hydrogen bonding. Optimised electrostatic parameters are displayed in figure 6.

Free energy and electrode potential results

Free energy results from the solution phase mutations, both molecular and electrostatic, are given in table 5. Overall solution phase free energy changes were calculated by averaging the results from forward and backward perturbation runs.

In all cases it can be seen that hystereses between forward and backward perturbations are small indicating the efficiency of phase space sampling in all simulations. Standard deviations on incremental free energy changes for individual simulation windows in all perturbations were small (< 10% of the free energy change per window, average) indicating good convergence of calculated free energy changes. Dihedral angle distributions for para-hydrobenzoquinone and coupled dihedral angle distributions for ortho-hydrobenzoquinone show that although sampling over torsional phase space was not exhaustive, torsional space was sampled correctly according to the energy expression employed for the particular system in question. Analysis of dihedral and coupled dihedral angle distribution in all mutations involving hydrobenzoquinones, through the FEP equation, was used to assess the intramolecular torsional contribution to calculated free energy changes. These values are also displayed in table 5.

Intramolecular contributions to solution phase free energy changes for both ortho and para molecular perturbations show good agreement between simulations involving different electrostatic parameter sets (3-21G and SOPLS derived). This agreement indicates torsional sampling in these simulations has been thorough within the energetically allowed regions of torsional space. Furthermore, in the case of the para system this intramolecular contribution (-6.58 kJmol^{-1} for 3-21G electrostatic parameters and -6.96 kJmol^{-1} for SOPLS optimised electrostatic parameters) is very similar to the free energy change for the gas phase perturbation, 6.86 kJmol^{-1} . This similarity demonstrates similar torsional sampling in both gas and solution phase simulations. The

Table 5 *Solution phase free energy results and intramolecular torsional contributions to them for molecular perturbations (hydroquinone -> quinone) and electrostatic perturbations.*

Mutation (electrostatic parameters)		ΔΔG [$kJmol^{-1}$] (inter + intra)	Intramolecular contribution [$kJmol^{-1}$]	ΔΔG [$kJmol^{-1}$] (inter only)
2hpbq -> pbq, (3-21G)		19.73 ± 0.5	-6.58	26.31
2hobq -> obq, (3-21G)		12.86 ± 041	-11.52	24.38
2hpbq -> pbq, (SOPLS)		4.55 ± 1.22	-6.96	11.51
2hobq -> obq, (SOPLS)		-17.89 ± 1.80	-11.12	-6.77
3-21G -> STO3G	2hpbq	31.58 ± 0.35	negligible	31.58
	pbq	19.07 ± 0.34	negligible	19.07
	2hobq	33.14 ± 0.39	negligible	33.14
	obq	20.79 ± 0.25	negligible	20.79
2hpbq -> pbq, (STO-3G)		7.22	-6.58	13.80
2hobq -> obq, (STO-3G)		0.51	-11.52	12.03
3-21G -> 6-31G*	2hpbq	-3.54 ± 0.01	negligible	-3.54
	pbq	-13.98 ± 0.18	negligible	-13.98
	2hobq	0.12 ± 0.10	negligible	0.12
	obq	-11.97 ± 0.16	negligible	-11.97
2hpbq -> pbq, (6-31G*)		9.29	-6.58	15.87
2hobq -> obq, (6-31G*)		0.77	-11.52	12.29

intramolecular torsional contributions to the difference in solvation free energies between ortho-hydrobenzoquinone and ortho-benzoquinone are some 4.04 $kJmol^{-1}$ and 3.63 $kJmol^{-1}$ (for perturbations involving 3-21G and SOPLS derived electrostatic parameters respectively) greater in magnitude than the free energy result from the ortho system gas phase perturbation. The discrepancy between the gas and solution phase values is indicative of differing torsional sampling in the gas and solution phases. Indeed, examination of the coupled dihedral angle distributions from the gas and solution phase simulations revealed more extensive torsional sampling in the gas phase simulation.

In general, the intramolecular torsional contributions to the differences in solvation free energies derived from the dihedral angle distributions favours the oxidised, quinone, form.

Analysis of dihedral angle distributions from electrostatic perturbations involving hydrobenzoquinones revealed negligible intramolecular contributions to charge mutations free energy changes. This result was expected as the torsional parameterisation of the hydroquinones remains constant throughout the charge perturbations. Furthermore, alteration in sampling of torsional phase space due to changes in electrostatic parameterisation appears to be insignificant. Thus, calculated charge mutation free energies could be combined directly with differences in solvation free energies calculated through the earlier molecular mutations to ascertain the effect on solvation free energies differences of altering electrostatic parameterisation.

Differences in solvation free energies (ΔG_3 - ΔG_1 and ΔG_2 - ΔG_4 from the thermodynamic cycle, figure 1) between the quinones and there respective reduced forms, as described by different electrostatic parameters, were found by subtracting the intramolecular torsional contribution from calculated free energy changes.

Free energy results show, in general, that solvation appears to stabilise the hydroquinone over the quinone form. Only for the ortho quinone system where electrostatics are described by optimised electrostatic parameters is this found not to be the case. It can be seen from table 5 that the calculated difference in solvation free energies between the quinones and their reduced forms varies quite considerably depending on the elctrostatic parameters employed. This results demonstrates the sensitive dependence of FEP calculated free energy changes on electrostatic parameterisation. It is also apparent that when electrostatic parameters derived from *ab initio* derived MEPs are employed in solution phase simulations the difference between the solvation free energy differences calculated for ortho and para-benzoquinones remains almost constant (1.77 $kJmol^{-1}$, 1.93 $kJmol^{-1}$ and 3.58

kJmol^{-1} for STO-3G, 3-21G and 6-31G* derived charges respectively). This same quantity found from perturbations involving the SOPLS optimised electrostatic parameters is calculated as 18.28 kJmol^{-1}. Thus it appears that calculated differences in solvation free energies are merely scaled by the alteration of electrostatic parameters derived from one *ab initio* basis set to another.

Differences in reduction potentials, ΔE, between ortho and para-benzoquinones, as calculated through equations 1 and 2 are displayed along with the experimental value in table 6.

It is apparent from table 6 that electrode potential results generally in best agreement with experiment are those found when $\Delta\Delta G_{gas}$ is calculated employing RHF/STO-3G *ab initio* calculations and atom centred charges derived from *ab initio* calculated MEPs are used in solution phase simulations. In these cases the average error in ΔE is 38.9 mV corresponding to an error in $\Delta\Delta G_{aq}$ (figure 1) of 7.5 kJmol^{-1}. Although these results seem reasonable the STO-3G basis set used to calculate the major contributant to $\Delta\Delta G_{gas}$ represents the lowest level of *ab initio* theory used in this study and therefore the least accurate. The agreement with experiment of results obtained from the combination of STO-3G $\Delta\Delta G_{gas}$ and *ab initio* derived electrostatic parameters has been tentatively ascribed to a cancellation of errors.

Electrode potential results derived from values of $\Delta\Delta G_{gas}$ found from RHF/3-21G, RHF/6-31G* and MP2/6-31G* calculations and simulations where *ab initio* derived electrostatic parameters have been employed show poor agreement with the experimental answer of -92.2 mV. The average error over these results is 120.9 mV corresponding to an error in $\Delta\Delta G_{aq}$ of 23.3 kJmol^{-1}. Of these results, those derived from use of the MP2/6-31G* value of $\Delta\Delta G_{gas}$ are in best agreement with experiment having an average error of 101.1 mV (corresponding to a 19.5 kJmol^{-1} error in $\Delta\Delta G_{aq}$). The MP2 level of *ab initio* theory in conjunction with the 6-31G* basis set should be capable of performing energy caclulations in good agreement with experiment on molecules as small as the quinones and hydroquinones and it was expected that use of MP2/6-31G* values for $\Delta\Delta G_{gas}$ would give the most accurate results. It is noticeable that, given a particular value of $\Delta\Delta G_{gas}$, the value of the calculated reduction potential shows little dependence on the basis set employed generate the electrostatic parameters through *ab initio* calculations. This demonstates that atom centred charges derived from different *ab initio* basis sets provide similar relative descriptions of the aqueous ortho-hydrobenzoquinone / para-benzoquinone and para-hydrobenzoquinone / ortho-benzoquinone systems. Overall, when *ab initio* CHELPG derived charges are employed to represent the electrostatic interactions of the quinone and hydroquinone molecules in aqueous solution, results obtained are in poor agreement with the experimental value.

Due to the high level of *ab initio* theory used in the MP2/6-31G* calculations it is assumed that errrors in the calculated value of $\Delta\Delta G_{aq}$ and hence ΔE are due to errors in the calculation of solvation free energy differences. Errors in the calculation of solvation free energy differences could be caused by either a poor sampling of phase space, poor convergence of free energy changes or the convergence of free energy changes to the wrong values. Given the small hystereses in calculated free energy changes and the small standard deviations on incremental free energy results it appears that it is the latter reason which accounts for the observed errors in calculated quantites. If this is the case then it appears that atom centred charges derived from *ab initio* wavefunctions using the CHELPG algorithm provide an inaccurate description of molecular electrostatics in aqueous solution.

Examination of the reduction potential results calculated using data from simulations where the SOPLS / optimised electrostatic parameters were employed shows a much better general agreement with experiment than do the other results. With the exception of the results derived using the RHF/STO-3G $\Delta\Delta G_{gas}$ value, all calculated values of ΔE lie within 52 mV of the experimental result. The best result is obtained when the value of $\Delta\Delta G_{gas}$ obtained from the MP2/6-31G* calculations is employed and is only 18.9 mV from the ex-

Table 6 *Calculated differences in reduction potentials between ortho and para-benzoquinones. Reduction potential results are shown for all different sets of electrostatic parameters employed in solution phase simulations and all different ab initio basis sets used in the calculation of* $\Delta\Delta G_{gas}$*. Also shown is the experimental value.*

Electrostatic parameters	**$\Delta\Delta G_{gas}$ (RHF/STO-3G)**	**$\Delta\Delta G_{gas}$ (RHF/3-21G)**	**$\Delta\Delta G_{gas}$ (RHF/6-31G*)**	**$\Delta\Delta G_{gas}$ (MP2/6-31G*)**
STO-3G MEP	-57.3 mV	-223.8 mV	-229.0 mV	-196.7 mV
3-21G MEP	-56.5 mV	-223.0 mV	-228.2 mV	-195.9 mV
6-31G* MEP	-47.9 mV	-214.4 mV	-219.6 mV	-187.3 mV
Optimised / SOPLS	+28.3 mV	-138.2 mV	-143.4 mV	-111.1 mV
Experimental [14]		-92.2 mV		

perimental value corresponding to an error in $\Delta\Delta G_{aq}$ of only 3.6 $kJmol^{-1}$.

Conclusions.

For the most part, the difference in solution phase reduction potentials between ortho and para-benzoquinones evaluated employing high level *ab initio* calculations and the free energy perturbation theory within Monte Carlo simulations shows poor agreement with the experimental value. This poor agreement arises due to the poor quality of the intermolecular force field parameters applied to describe the solute molecules in solution phase simulations. The best agreement betwen calculated and experimental reduction potential differences arises when electrostatic parameters derived specifically for the sytem in question are employed to describe solute molecules and *ab initio* calculations are performed at the MP2 level. Development of such parameters and the ensuing MC simulations constitute a time consuming process. It should be noted that the use of free energy perturbation theory within Monte Carlo simulations in conjunction with high level *ab initio* calculations is capable of producing results in good agreement with experiment. However, as a routine method of obtaining such quantities FEP theory is limited and more epeditious methods are required to allow the computation of solution phase reduction potentials to become routine.

Acknowledgements: D. R. L. would like to acknowledge the financial assistance of Lilly Research as part of a C. A. S. E studentship.

References.

1. N. Metropolis and S. Ulam, *J. A. Stat. Ass.*, **1949**, 44, 335.
2. M. P. Allen and D. J. Tildesley, *Computer Simulations of Liquids*, **1987**, Oxford University Press, Oxford, UK.
3. Torrie G. M. and Valleau J. P., *J. Comput. Phys.*, **1977**, 23, 187.
4. W. L. Jorgensen, *J. Phys. Chem.*, **1983**, 87, 5304.
5. W. L. Jorgensen, *BOSS (Version 2.8) Users Manual*, **1990**, Dept. of Chemistry, Yale University, New Haven, CT, USA.
6. W. L. Jorgensen and J. Tirado-Rives, *J. Am. Chem. Soc.*, **1988**, 110, 1657.
7. J. Paranata, S. J. Wierschke and W. L. Jorgensen, *J. Am. Chem. Soc.*, **1991**, 113, 2810.
8. W. L. Jorgensen, E. R. Laird, T. B. Nguyen and J. Tirado-Rives, *J. Comp. Chem.*, **1993**, 14, 206.
9. S. J. Weiner, P. A. Kollman, D. T. Nguyen and D. A. Case, *J. Comp. Chem.*, **1985**, 7, 230.
10. U. Burkert and N. L. Allinger, *ACS Monograph*, **1982**, 177.
11. C. M. Brenenman and K. B. Wiberg, *J. Comp. Chem.*, **1990**, 11, 361.
12. D. L Beveridge and F. M. DiCapua in *Computer Simulations of Biomolecular Systems: Theoretical and Experimental Applications.*, **1989**, Eds. W. F. van Gunsteren and P. K. Weiner, ESCOM, Leiden, The Netherlands.
13. D. G. Lister, J. N. MacDonald and N. L. Owen, *Internal rotation and inversion.*, **1978**, Academic Press Inc., London, UK.
14. H. W. Moore, *Science*, **1977**, 197, 527.
15 C. A. Reynolds, *J. Am. Chem Soc.*, **1990**, 112, 7545.
16. M. J. Frisch, M. Head-Gordon, H. B. Schlegel, K. Raghavachari, J. S. Binkley, C. Gonzales, D. J. Defrees, D. J. Fox, R. A. Whiteside, R. Seeger, C. F. Melius, J. Baker, R. Martin, L. R. Khann, J. J. P. Stewart, E. M. Fluder, S. Topiol and J. A. Pople, *Gaussian 92,* **1992**, Gaussian Inc., Pittsburgh, PA, USA.
17. W. J. Hehre, R. Ditschfield, R. F. Stewart and J. A. Pople, *J. Chem. Phys.*, **1969**, 52, 2769.
18. J. S. Binkley, J. A. Pople and W. J. Hehre, *J. Am. Chem. Soc.*, **1980**, 102, 939.
19. W. J. Hehre, R. Ditschfield and J. A. Pople, *J. Chem. Phys.*, **1972**, 56, 2257 and P. C. Hanrihanran and J. A. Pople, *Theor. Chim. Acta*., **1973**, 28, 213.
20. J. S. Binkley and J. A. Pople, *Int. J. Quant. Chem.*, **1975**, 9, 229.
21. M. J. S. Dewar, E. G. Zoebisch, E. F. Healy and J. J. P. Stewart, *J. Am. Chem.. Soc.*, **1985**, 107, 3902.
22. J. J. P. Stewart and F. J. Seiler, *MOPAC (Version 6)*, **1988**, United States Air Force Academy, Colorado Springs, CO, USA.
23. C. A. Reynolds in "*Computer Aided Molecular Design.*", **1989**, Ed. W. G. Richards, I. B. C., London, UK.
24. W. L. Jorgensen, *BOSS (Version 3.1)*, **1991**, Yale University, New Haven, CT. USA.
25. R. W. Zwanzig, *J. Chem. Phys.*, **1954**, 22, 1420.
26. W. L Jorgensen and D. L. Severance, *SOPLS*, **1994**, Yale University, New Haven, CT., USA.
27. W. L. Jorgensen, J. Chandresekhar, J. D Madura, R. W. Impey and M. L. Klein, *J. Chem. Phys.*, **1983**, 79, 926.
28. W. L. Jorgensen, *BOSS (Version 3.1) Users Manual., p 9*, **1991**, Yale University, New Haven, CT. USA.